ATMOSPHERIC AND OCEANIC SCIENCE LETTERS, 2013, VOL. 6, NO. 5, 343–348

Simulation of the Direct Radiative Effect of Mineral Dust and Sea Salt Aerosols in a Doubled Carbon Dioxide Climate

YUE Xu[1, 2, 3], LIAO Hong[4, 1], and TANG Jin-Ping[5, 6]

[1] *Climate Change Research Center, Chinese Academy of Sciences (CAS), Beijing 100029, China*
[2] *Nansen-Zhu International Research Center, Institute of Atmospheric Physics (IAP), CAS, Beijing 100029, China*
[3] *School of Engineering and Applied Sciences, Harvard University, Cambridge, Massachusetts 02143, USA*
[4] *State Key Laboratory of Atmospheric Boundary Layer Physics and Atmospheric Chemistry (LAPC), IAP, CAS, Beijing 100029, China*
[5] *Key Laboratory of Middle Atmosphere and Global Environment Observation, IAP, CAS, Beijing 100029, China*
[6] *University of CAS, Beijing 100049, China*

Received 14 December 2013; revised 22 January 2013; accepted 4 February 2013; published 16 September 2013

Abstract The authors examine the equilibrium climatic response to the direct radiative effect (DRE) of mineral dust and sea salt aerosols in a doubled-CO_2 climate with two-way coupling of aerosol-climate interactions. In response to the drier and windier conditions, dust emissions increase by 26% in the Sahara Desert and by 18% on the global scale relative to present day. Sea salt emissions increase in high latitudes (>60°) but decrease in middle latitudes (30°–60°) of both hemispheres due to the poleward shift of westerlies, leading to a 3% decrease in global emissions. The burdens of dust and sea salt increase by 31% and 7% respectively, because reductions in rainfall over the tropical oceans increase the lifetime of particles in the warmer climate. The higher aerosol loading in the doubled-CO_2 climate reinforces aerosol DRE by -0.2 W m^{-2}, leading to an additional cooling of 0.1°C at the surface compared with the climatic effects of aerosols in present day. The additional cooling from changes in natural aerosols compensates for up to 15% of the regional warming induced by doubled CO_2.

Keywords: mineral dust, sea salt aerosol, direct radiative effect

Citation: Yue, X., H. Liao, and J.-P. Tang, 2013: Simulation of the direct radiative effect of mineral dust and sea salt aerosols in a doubled carbon dioxide climate, *Atmos. Oceanic Sci. Lett.*, **6**, 343–348, doi:10.3878/j.issn.1674-2834.12.0107.

1 Introduction

Mineral dust and sea salt aerosols play important roles in the Earth System. Every year, approximately 1000–3000 teragrams (Tg, 10^{12} g) of dust is blown into the atmosphere over land surfaces (Penner et al., 2001), and 1000–10000 Tg of sea salt is emitted from the oceans (Blanchard et al., 1985). The suspended aerosols influence climate by scattering and absorbing both shortwave and longwave radiation (Miller and Tegen, 1998; Ayash et al., 2008), and the altered climate can in turn influences the emission, transport, and deposition of the aerosols (Miller et al., 2004; Yue et al., 2010).

Modeling studies have simulated the direct radiative effects (DRE) of mineral dust and sea salt in the present-day atmosphere. More than 10 studies, summarized in Yue et al. (2010), have estimated that the net (shortwave plus longwave) DRE of dust at the top of atmosphere (TOA) is in the range of -0.5 to approximately $+0.4$ W m^{-2}. The high sensitivity of DRE to the parameters of the aerosol itself and to atmospheric conditions makes the sign of dust effects uncertain (Liao and Seinfeld, 1998). In response to DRE of dust, the global mean surface air temperature is predicted to decrease by 0.1°C, with regional cooling of up to 1°C (Miller and Tegen, 1998). On the other hand, a number of studies have estimated a global average shortwave DRE from -0.3 to -1.1 W m^{-2} for sea salt, resulting in a decrease of 0.5°C in the global mean surface air temperature (Yue et al., 2012). Mineral dust and sea salt aerosols were found to contribute to aridity during glacial periods, when aerosol loading was much higher relative to present day (DeAngelis et al., 1997). However, few studies have quantified the impacts of these natural aerosols in the global warming background, especially when the warming trend has been accelerating in recent decades (Trenberth et al., 2007).

In this study, we investigate the climatic response to the DRE of mineral dust and sea salt aerosols in a doubled-CO_2 climate using a general circulation model (GCM) with two-way aerosol-climate coupling. We pay particular attention to (1) the changes in aerosol cycles that result from changes in meteorological fields, and (2) the direct radiative feedback of such changes on mineral dust and sea salt in the future climate.

2 Model and simulations

We use the IAP grid-point nine-layer atmospheric general circulation model (IAP9L-AGCM) to perform the numerical simulations. The model has a horizontal resolution of 4° latitude by 5° longitude, with nine vertical layers up to 10 hPa (Zhang, 1990). The GCM is coupled with a mixed layer ocean model from Hansen et al. (1984) and utilizes an annual mean mixed layer depth derived from Levitus et al. (2000). We estimate *Q* flux based on the energy balance between the predicted net atmosphere-to-

---

Corresponding author: LIAO Hong, hongliao@mail.iap.ac.cn

ocean heat flux and the water heat content within the oceanic mixed layer, calculated with observed sea surface temperature (SST). We assume that the *Q* flux remains constant for the present day and doubled-CO_2 climate. The online simulation of mineral dust aerosol was integrated into the GCM by Yue et al. (2009) and further updated to simulate sea salt aerosol in Yue et al. (2012). The model simulates four size bins of dust and six size bins of sea salt with dry radii of both aerosols ranging from 0.1 to 10 μm. The dust emission scheme follows Wang et al. (2000), which calculates dust uplift flux as a function of friction velocity and relative humidity of surface air. The generation of sea salt is parameterized as a function of wind speed at 10 m, following the schemes of Monahan et al. (1986), Smith et al. (1993), and Gong (2003) for different size bins. Dry deposition of particles is dependent on both gravity and turbulent mixing. For wet deposition, we consider rainfall scavenging, which is determined by precipitation rate and size-dependent empirical constants. The simulated cycles of dust and sea salt, including surface concentrations and optical depths, have been evaluated in Yue (2009) and Yue and Liao (2012).

The GCM simulates both shortwave and longwave radiative effects of aerosols. For the shortwave spectra, we calculate aerosol optical thickness, single scattering albedo (SSA), and asymmetry factor using the Mie theory (de Rooij and van der Stap, 1984). We use the refractive index from Woodward (2001) for dust aerosol, and that from Hess et al. (1998) for sea salt. The calculated dust SSA is approximately 0.89 at 0.55 μm over the Sahara Desert, which is much lower than the estimates of 0.95–0.97 from observations (Kauffman et al., 2001; Dubovik et al., 2002). Although some studies found low SSA for dust over Asia (e.g. Zhang et al., 2010), the global average is dominated by dust emitted from the Sahara Desert. As a result, we manually increase the SSA by 8% to reduce the strong absorption by dust. However, we discuss the results with the original dust SSA as reference. For the longwave bands, we calculate aerosol transmission using an exponential approximation scheme proposed by Carlson and Benjamin (1980).

We perform four climate simulations to examine the climatic responses to the DRE of dust and sea salt in a doubled-CO_2 climate (Table 1). Simulations PRND_CTRL and PRND_AER are performed for present-day conditions. The CO_2 concentrations in these simulations are set to 360 ppm, which was the greenhouse gas (GHG) level in 1995. PRND_CTRL simulates aerosol cycles but omits their DRE. The simulation PRND_AER considers the interactions between climate and aerosols; the dust and sea salt particles influence radiative fluxes while the perturbed climate in turn affects the aerosol budget. The differences between PRND_AER and PRND_CTRL represent the climatic responses to aerosol DRE in the present day. Similarly, we perform simulations DCO2_CTRL and DCO2_AER to quantify the DRE of aerosols in an equilibrium climate with doubled CO_2 concentration. The CO_2 concentration for DCO2 simulations is set to 720 ppm, which is the predicted GHG level in 2100 following the A1B scenario from the Intergovernmental Panel on Climate Change (IPCC) Fourth Assessment Report (AR4) database. In these two simulations, we use monthly sea ice temperatures derived from the median surface temperatures simulated by the 17 IPCC climate models for the equilibrium A1B scenario. Each climate simulation runs for 50 years, and the average values over the last 30 years are presented in the next sections.

Table 1 Summary of climate simulations.

Simulation	Description
PRND_CTRL	Present-day climate with dust and sea salt cycles; No aerosol DRE
PRND_AER	Present-day climate with dust and sea salt cycles; Interactive aerosol DRE
DCO2_CTRL	Doubled-CO_2 climate with dust and sea salt cycles; No aerosol DRE
DCO2_AER	Doubled-CO_2 climate with dust and sea salt cycles; Interactive aerosol DRE

3 Results

3.1 Simulated changes in climate

Figure 1 shows the simulated changes in meteorological fields from the present day to the doubled-CO_2 atmosphere. The surface air temperature shows a general increase, with large values exceeding 3°C over the continents. A strong warming is found at the Arctic as a result of the reduced sea ice area. Global precipitation shows an increase of 0.15 mm d^{-1} with regional changes of both signs. A significant increase in rainfall is predicted at high latitudes, due to the strengthened moisture convergence in these areas (Bosilovich et al., 2005). However, decreases in precipitation are predicted over some subtropical oceans, as a consequence of the intensified and poleward expansion of subtropical highs (Meehl et al., 2007). Rainfall exhibits significant decreases over northern Africa and the Arabian area, following the increased moisture divergence and a systematic poleward shift of storm track, which affects moisture transport (Christensen et al., 2007). Both the changes in temperature and precipitation resemble those simulated with multi-model ensembles as shown in Meehl et al. (2007).

Relative humidity of surface air exhibits uniform increases over open oceans, because the more-abundant rainfall outweighs the increased evaporation by strong surface warming (Fig. 1a). However, over Africa, the combined effects of reduced precipitation (Fig. 1b) and enhanced evaporation result in a widespread decrease in relative humidity. A similar drought tendency over North Africa is also reported in Meehl et al. (2007) based on the multi-model ensemble. Wind speed increases in Africa, South Asia, and South America but decreases over other continents. Over the oceans, the wind intensifies in the tropical Atlantic but weakens over the Pacific. A poleward shift of westerlies is predicted over the Southern Oceans, which can be explained by the expansion of meridional circulations (Yin, 2005) and is consistent with the multi-model projections by McInnes et al. (2011).

3.2 Simulated changes in aerosol cycles

Most dust emissions are confined to arid and semi-arid regions in the Northern Hemisphere, with the maximum emissions over the Sahara Desert (Fig. 2a). In a doubled-CO_2 climate, the Saharan source is intensified by 26% (Fig. 2b), due to the drier (Fig. 1c) and windier (Fig. 1d) conditions. On the other hand, dust emissions in central Asia are weakened by 12% (Fig. 2b), as a result of increased precipitation (Fig. 1b) and decreased wind speed (Fig. 1d). On a global scale, annual dust emissions increase by 18% in the doubled-CO_2 climate (Table 2). In addition, the decrease in rainfall over North Africa reduces wet scavenging of dust particles, resulting in an increase in aerosol loading and lifetime (Table 2).

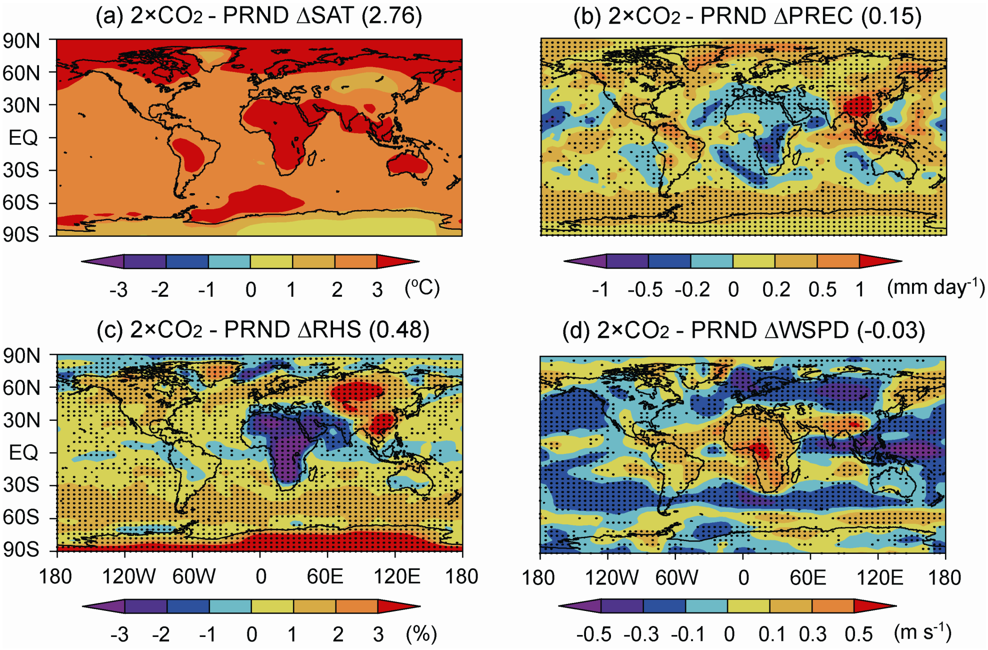

Figure 1 Simulated changes in (a) surface air temperature, (b) precipitation, (c) surface relative humidity, and (d) surface wind speed in the doubled-CO_2 climate relative to present day. Results are calculated as the differences between simulations DCO2_CTRL and PRND_CTRL. Differences that pass the 95% confidence level test are denoted with dots. No dots are indicated for (a) because the changes are significant over every grid box. The globally averaged changes are shown in brackets.

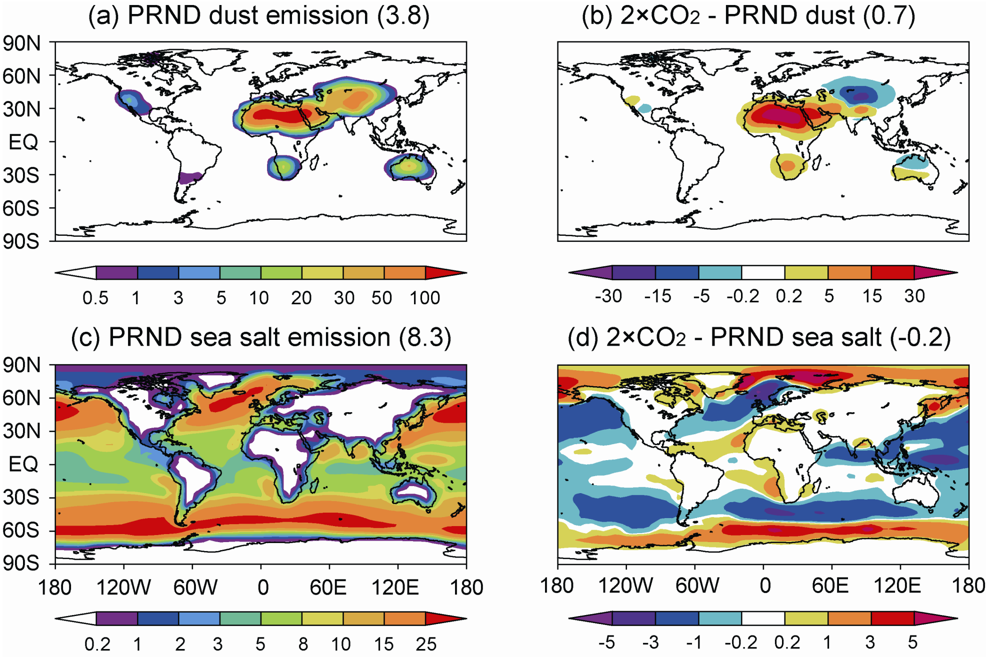

Figure 2 Simulated (a) dust and (c) sea salt aerosol emissions in present day, and (b, d) their changes in a doubled-CO_2 climate. Results for (a) and (c) are from simulation PRND_CTRL. Results for (b) and (d) are calculated as the differences between simulations DCO2_CTRL and PRND_CTRL. The globally averaged values are shown in brackets. Units: g m^{-2} yr^{-1}.

Table 2 Comparison of aerosol budgets in the present day and doubled-CO_2 climates.

	PRND_CTRL	DCO2_CTRL
Dust emission (Tg yr^{-1})	1925	2264
Dust burden (Tg)	27.7	36.4
Dust lifetime (days)	5.3	5.9
Sea salt emission (Tg yr^{-1})	4249	4143
Sea salt burden (Tg)	8.1	8.7
Sea salt lifetime (days)	0.7	0.8

Sea salt emission is efficient at high latitudes of both hemispheres (Fig. 2c). In the doubled-CO_2 climate, the poleward shift of westerlies enhances sea salt emissions over the Southern Ocean and the Arctic Ocean but reduces the emissions at mid-high latitudes (Fig. 2d). In addition, the melting of sea ice partly contributes to the increase of aerosol emissions at high latitudes. In tropical regions, sea salt aerosol emissions increase in the Atlantic but decrease in the Pacific, following changes in wind speed (Fig. 1d). On a global scale, a 3% decrease in sea salt emission is predicted in the warmer climate relative to present day (Table 2), similar to the 4% decrease estimated by Mahowald et al. (2006a). However, the sea salt burden increases by 7% because most floating particles locate at tropical areas where precipitation is projected to decline (Fig. 1b). As a result, the global mean lifetime of sea salt aerosol increases by 9%.

3.3 Simulated changes in aerosol DRE

Figure 3a shows the net (shortwave plus longwave) DRE of dust and sea salt at TOA for present day. Strong negative DREs are predicted over the tropical Atlantic and the Arabian Sea, a composite result of dust and sea salt radiative effects (Yue et al., 2010; Yue and Liao, 2012). In other oceanic areas, sea salt aerosol exerts a uniform cooling of approximately -1 W m^{-2}. Negative DREs are also predicted over most continents; however, the cooling is weak over the Sahara Desert, since the absorption of shortwave radiative fluxes by dust partly compensates for its scattering effect. On the global scale, dust and sea salt aerosols induce average DREs of -0.62 and -0.89 W m^{-2} respectively, leading to a total DRE of -1.51 W m^{-2} (Fig. 3a). However, using the original SSA value, dust aerosol leads to a positive DRE of 0.1 W m^{-2} due to high absorption over the Sahara Desert (not shown).

In the doubled-CO_2 climate, the negative DRE is reinforced in the tropical regions (Fig. 3b), due to the increased aerosol burdens in these areas. However, the cooling is weakened over central Asia as a result of decreases in regional dust emissions (Fig. 2b). For a similar reason, the negative DRE is weaker over 30–60°S, following changes in sea salt emissions (Fig. 2d). On an annual global mean basis, mineral dust and sea salt aerosols induce an additional cooling of 0.19 W m^{-2} in the doubled-CO_2 climate, to which changes in dust aerosol alone contribute 0.11 W m^{-2}. However, simulations using the original SSA predict the dust-induced cooling will intensify by only 0.02 W m^{-2} (not shown).

We also investigate temperature responses to the aerosol DRE. In present day, natural aerosols cause an annual and global mean cooling of 0.85°C, with the maximum cooling of 1.5°C occurring in tropical regions (Fig. 3c). The annual and global mean cooling by dust and sea salt is reinforced by 0.1°C in the doubled-CO_2 climate, with

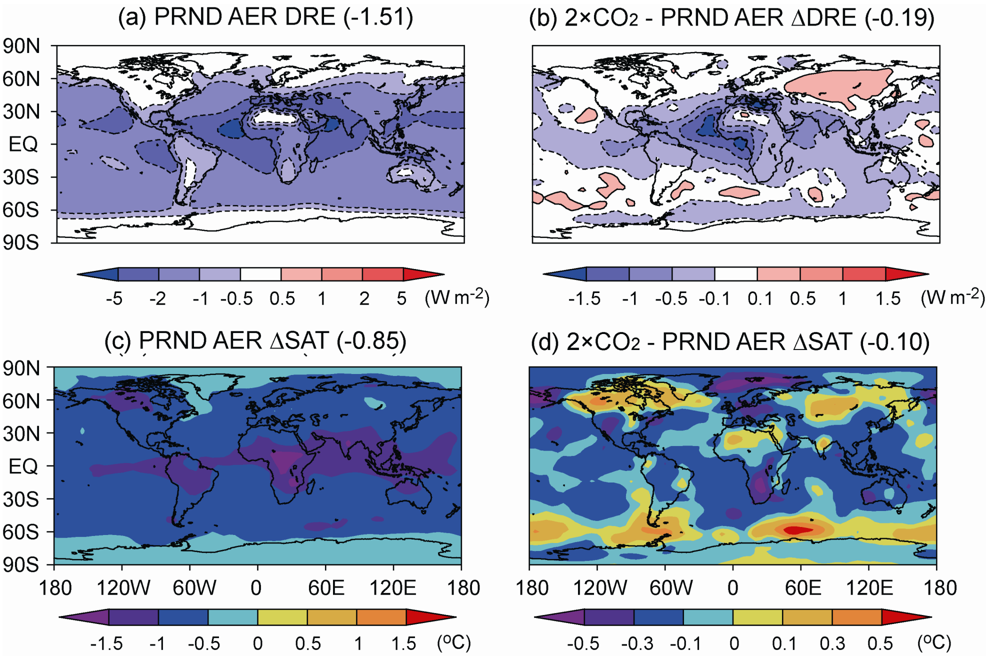

Figure 3 Simulated present-day (a) direct radiative effect (DRE) of dust plus sea salt aerosol at the top of atmosphere, and (b) its change in a doubled-CO_2 climate. The predicted temperature response to the aerosol DRE and its change in a doubled-CO_2 climate are shown in (c) and (d). Results for (a) and (c) are calculated as the differences between simulations PRND_AER and PRND_CTRL. Results for (b) and (d) are calculated as (DCO2_AER–DCO2_CTRL)–(PRND_AER–PRND_CTRL). The globally averaged values are shown in brackets.

an enhanced cooling of approximately 0.2°C in tropical oceans (Fig. 3d). Although such cooling by dust and sea salt only accounts for 4% of the warming caused by CO_2 on a global scale (Fig. 1a), regional effects may compensate the warming as much as 8%–15% over some tropical oceans (not shown).

4 Discussion and conclusions

We investigate climatic responses to the DRE of dust and sea salt aerosols in both present day and a doubled-CO_2 climate. Relative to present day, global dust emissions in the warmer climate increase by 18%, with the largest increase (26%) over the Sahara Desert. The global dust burden increases by 31% as a result of the enhanced emissions and weakened precipitation. Sea salt emissions are projected to decrease by 3% globally, as a combined result of increased emissions in high latitudes (>60°) and decreased emissions in middle latitudes (30°–60°) due to the poleward shift of westerlies. However, the sea salt burden increases by 7% because the weakened hydrologic cycle enhances the lifetime of particles over the tropical regions. In response to the changes in aerosol burdens from present day to the doubled-CO_2 climate, the global and annual mean DRE of dust and sea salt aerosols is reinforced from -1.5 to -1.7 W m^{-2}, leading to an additional cooling of 0.1°C at the surface. Such additional cooling can compensate for up to 15% of the warming induced by greenhouse gases over the tropical oceans. Our simulations suggest that the DRE of natural aerosols cannot be neglected in future climate simulations.

One of the limits of this study is that we do not account for the impact of the changes in source area on dust emission. For example, Mahowald et al. (2006b) estimated that global dust loading will decrease by 60% in the doubled-CO_2 climate, due to reductions in desert area resulting from the CO_2 fertilization effect. In addition, we omit the indirect effects of aerosols. Observations have shown that both mineral dust and sea salt can act as cloud condensation nuclei (Lohmann and Feichter, 2005; Twohy et al., 2009), leading to changes in cloud radiative forcing and precipitation. Further consideration of both changes in dust source and indirect effects of aerosols will better quantify the role of these natural aerosols in a future, warmer climate.

Acknowledgements. This research was supported by the National Basic Research Program of China (973 program, Grant 2010CB 951901) and the Strategic Priority Research Program of the Chinese Academy of Sciences (Grant XDA05100503).

References

Ayash, T., S. Gong, and C. Q. Jia, 2008: Direct and indirect shortwave radiative effects of sea salt aerosols, *J. Climate*, **21**, 3207–3220.

Blanchard, D. C., 1985: The oceanic production of atmospheric sea salt, *J. Geophys. Res.*, **90**, 961–963.

Bosilovich, M. G., S. D. Schubert, and G. K. Walker, 2005: Global changes of the water cycle intensity, *J. Climate*, **18**, 1591–1608.

Carlson, T. N., and S. G. Benjamin, 1980: Radiative heating rates for Saharan dust, *J. Atmos. Sci.*, **37**(1), 193–213.

Christensen, J. H., B. Hewitson, A. Busuioc, et al., 2007: Regional climate projections, in: *Climate Change 2007: The Physical Science Basis. Contribution of Working Group I to the Fourth Assessment Report of the Intergovernmental Panel on Climate Change*, C. Fu and F. Giorgi (Eds.), Cambridge University Press, Cambridge and New York, 129–234.

DeAngelis, M., J. P. Steffensen, M. Legrand, et al., 1997: Primary aerosol (sea salt and soil dust) deposited in Greenland ice during the last climatic cycle: Comparison with east Antarctic records, *J. Geophys. Res.*, **102**, 26681–26698.

de Rooij, W. A., and C. C. A. H. van der Stap, 1984: Expansion of Mie scattering matrices in generalized spherical functions, *Astron. Astrophys.*, **131**, 237–248.

Dubovik, O., B. Holben, T. F. Eck, et al., 2002: Variability of absorption and optical properties of key aerosol types observed in worldwide locations, *J. Atmos. Sci.*, **59**(3), 590–608.

Gong, S. L., 2003: A parameterization of sea-salt aerosol source function for sub- and super-micron particles, *Glob. Biogeochem. Cycles*, **17**(4), 1097, doi:10.1029/2003GB002079.

Hansen, J., A. Lacis, D. Rind, et al., 1984: Climate sensitivity: Analysis of feedback mechanisms, in: *Climate Processes and Climate Sensitivity*, *Geophys. Monogr. Ser.*, **29**, 130–163.

Hess, M., P. Koepke, and I. Schult, 1998: Optical properties of aerosols and clouds: The software package OPAC, *Bull. Amer. Meteor. Soc.*, **79**(5), 831–844.

Kaufman, Y. J., D. Tanré, O. Dubovik, et al., 2001: Absorption of sunlight by dust as inferred from satellite and ground-based remote sensing, *Geophys. Res. Lett.*, **28**(8), 1479–1482, doi:10.1029/2000GL012647.

Levitus, S., J. I. Antonov, T. P. Boyer, et al., 2000: Warming of the world ocean, *Science*, **287**, 2225–2229, doi:10.1126/science.287.5461.2225.

Liao, H., and J. H. Seinfeld, 1998: Radiative forcing by mineral dust aerosols: Sensitivity to key variables, *J. Geophys. Res.*, **103**(D24), 31637–31645.

Lohmann, U., and J. Feichter, 2005: Global indirect aerosol effects: A review, *Atmos. Chem. Phys.*, **5**, 715–737.

Mahowald, N. M., J. F. Lamarque, X. X. Tie, et al., 2006a: Sea-salt aerosol response to climate change: Last glacial maximum, preindustrial, and doubled carbon dioxide climates, *J. Geophys. Res.*, **111**(D5), D05303, doi:10.1029/2005JD006459.

Mahowald, N. M., D. R. Muhs, S. Levis, et al., 2006b: Change in atmospheric mineral aerosols in response to climate: Last glacial period, preindustrial, modern, and doubled carbon dioxide climates, *J. Geophys. Res.*, **111**, D10202, doi:10.1029/2005JD 006653.

McInnes, K. L., T. A. Erwin, and J. M. Bathols, 2011: Global climate model projected changes in 10 m wind speed and direction due to anthropogenic climate change, *Atmos. Sci. Lett.*, **12**(4), doi:10.1002/asl.341.

Meehl, G. A., T. F. Stocker, W. D. Collins, et al., 2007: Global Climate Projections, in: *Climate Change 2007: The Physical Science Basis. Contribution of Working Group I to the Fourth Assessment Report of the Intergovernmental Panel on Climate Change*, M. Allen and G. B. Pant (Eds.), Cambridge University Press, Cambridge and New York, 747–845.

Miller, R. L., J. Perlwitz, and I. Tegen, 2004: Feedback upon dust emission by dust radiative forcing through the planetary boundary layer, *J. Geophys. Res.*, **109**, D24209, doi:10.1029/2004JD 004912.

Miller, R. L., and I. Tegen, 1998: Climate response to soil dust aerosols, *J. Climate*, **11**, 3247–3267.

Monahan, E. C., D. E. Spiel, and K. L. Davidson, 1986: A model of marine aerosol generation via whitecaps and wave disruption, in: *Oceanic Whitecaps and Their Role in Air-Sea Exchange Processes*, E. C. Monahan and G. i. M. Niocaill (Eds.), Springer Netherland, Dordrecht, 167–174.

Penner, J. E., M. Andreae, H. Annegarn, et al., 2001: Aerosols:

Their direct and indirect effects, in: *Climate Change 2001: The Scientific Basis, Contribution of Working Group I to the Third Assessment Report of the Intergovernmental Panel on Climate Change*, B. Nyenzi and J. Prospero (Eds.), Cambridge University Press, Cambridge and New York, 291–336.

Smith, M. H., P. M. Park, and I. E. Consterdine, 1993: Marine aerosol concentration and estimated fluxes over sea, *Quart. J. Roy. Meteor. Soc*, **119**, 809–824.

Trenberth, K. E., P. D. Jones, P. Ambenje, et al., 2007: Observations: Surface and atmospheric climate change, in: *Climate Change 2007: The Physical Science Basis. Contribution of Working Group I to the Fourth Assessment Report of the Intergovernmental Panel on Climate Change*, B. J. Hoskins et al. (Eds.), Cambridge University Press, Cambridge and New York, 235–336.

Twohy, C. H., S. M. Kreidenweis, T. Eidhammer, et al., 2009: Saharan dust particles nucleate droplets in eastern Atlantic clouds, *Geophys. Res. Lett.*, **36**, L01807, doi:10.1029/2008GL035846.

Wang, Z., H. Ueda, and M. Huang, 2000: A deflation module for use in modeling long-range transport of yellow sand over East Asia, *J. Geophys. Res.*, **105**(D22), 26947–26959.

Woodward, S., 2001: Modeling the atmospheric life cycle and radiative impact of mineral dust in the Hadley Centre climate model, *J. Geophys. Res.*, **106**(D16), 18155–18166, doi:10.1029/2000JD900795.

Yin, J. H., 2005: A consistent poleward shift of the storm tracks in simulations of 21st century climate, *Geophys. Res. Lett.*, **32**, L18701, doi:10.1029/2005GL023684.

Yue, X., and H. Liao, 2012: Climatic responses to the shortwave and longwave direct radiative effects of sea salt aerosol in present day and the last glacial maximum, *Climate Dyn.*, **39**(12), 3019–3040, doi:10.1007/s00382-012-1312-5.

Yue, X., H. J. Wang, H. Liao, et al., 2010: Simulation of dust aerosol radiative feedback using the GMOD: 2. Dust-climate interactions, *J. Geophys. Res.*, **115**, D04201, doi:10.1029/2009JD012063.

Yue, X., H. J. Wang, Z. F. Wang, et al., 2009: Simulation of dust aerosol radiative feedback using the global transport model of dust: 1. Dust cycle and validation, *J. Geophys. Res.*, **114**, D10202, doi:10.1029/2008JD010995.

Zhang, L., X. Cao, J. Bao, et al., 2010: A case study of dust aerosol radiative properties over Lanzhou, China, *Atmos. Chem. Phys.*, **10**, 4283–4293.

Zhang, X., 1990: Dynamical framework of IAP nine-level atmospheric general circulation model, *Adv. Atmos. Sci.*, **7**(1), 67–77, doi:10.1007/BF02919169.